



# Longwave Measurements for the Coast of British Columbia and Improvements to the Tsunami Warning Capability

ALEXANDER B. RABINOVICH<sup>1,2</sup> and FRED E. STEPHENSON<sup>3</sup>

<sup>1</sup>*Fisheries and Oceans Canada, Ocean Sciences and Productivity, Institute of Ocean Sciences, 9860 West Saanich Road, Sidney, B.C., V8L 4B2 Canada (E-mail: RabinovichA@pac.dfo-mpo.gc.ca);*

<sup>2</sup>*Russian Academy of Sciences, P.P. Shirshov Institute of Oceanology, 36 Nakhimovsky Prosp., Moscow, 117851 Russia (E-mail: abr@iki.rssi.ru);*

<sup>3</sup>*Fisheries and Oceans Canada, Canadian Hydrographic Service, Institute of Ocean Sciences, 9860 West Saanich Road, Sidney, B.C., V8L 4B2 Canada (E-mail: StephensonF@pac.dfo-mpo.gc.ca)*

(Received: 13 June 2002; in final form: 27 May 2003)

**Abstract.** A few years ago the Canadian Hydrographic Service initiated a major upgrade to all tide gauges and tsunami stations on the coast of British Columbia (B.C.). This program was undertaken to address shortcomings of the earlier digital systems and was driven by concerns about emergency response continuity in the year 2000. By 1999, thirteen tide gauge stations had been installed and were operational. Three of these stations (Tofino, Winter Harbour, and Langara) were selected for use as tsunami warning stations. Several years of continuous, high quality data have now been collected at these stations and used for analysis of long waves in the tsunami frequency band. Careful examination of these data revealed two weak tsunamis recorded by several B.C. stations: a distant tsunami of June 23, 2001 generated by the Peru Earthquake ( $M_w = 8.4$ ), and a local tsunami of October 12, 2001 induced by the Queen Charlotte Earthquake ( $M_w = 6.3$ ). Spectral characteristics of these two tsunamis are compared with the spectral characteristics of long waves generated by a strong storm (October, 2000) and of ordinary background oscillations. The topographic admittance functions (frequency responses) constructed for all stations showed that most of them (in particular, Winter Harbour, Tofino, Bamfield, Port Hardy, and Victoria) have strong resonance at periods from 2.5 to 20 min, indicating that these locations are vulnerable to relatively high-frequency tsunamis. The Winter Harbour station also has two strong resonant peaks with periods of 30 and 47 min and with amplification factors of about 7. The estimated source functions show very clear differences between long waves associated with the seismic source (typical periods 10–30 min) and those generated by a storm, which typically have shorter periods and strong energy pumping from high-frequencies due to non-linear interaction of wind waves.

**Key words:** tsunami, long waves, seiches, tide gauge, spectral analysis, tsunami warning, British Columbia coast, Vancouver Island, meteorological tsunamis, edge waves, infragravity waves.

## 1. Introduction

The coast of British Columbia extends from approximately 48° N to 55° N, a distance of about 775 km. However, this coast is a complex network of inlets, straits, passes, sounds, and narrows which has a coastline, including islands, of

approximately 27,300 km (Thomson, 1981). Significant parts of this coastline are susceptible to the effects of tsunamis generated within the Pacific basin (Rapatz and Murty, 1987; Murty, 1992; Clague *et al.*, 2003). Geological and geophysical evidence gathered along the western coastline of Vancouver Island, as well as on the Washington and Oregon coasts, show that major Cascadia earthquakes accompanied by destructive tsunamis have an average recurrence of 500 years in this region (Clague and Bobrowsky, 1999; Clague *et al.*, 2003). Trans-Pacific tsunamis caused by major earthquakes in the Pacific “Rim of Fire” can also significantly affect the B.C. coast (Murty, 1992; Clague, 2001). The March 1964 Alaska earthquake with magnitude  $M_w = 9.2$  produced a catastrophic tsunami which swept southward from the source area (Prince William Sound, Alaska) along the British Columbia coast causing about \$10 million in damage (1964 dollars) (Wigen and White, 1964; Murty, 1977; Clague, 2001; Clague *et al.*, 2003). According to Rapatz and Murty (1987) and Hebenstreit and Murty (1989) for the coast of British Columbia there is also a high potential risk of destructive tsunamis caused by local major earthquakes in the region of Puget Sound and Juan de Fuca Strait.

The Pacific Tsunami Warning Center (PTWC), which was established by the UNESCO International Oceanographic Commission (IOC) in 1946, is designed to detect tsunamis and provide prompt notification of a tsunami threat to member states of the International Tsunami Warning System for the Pacific (ITSU). British Columbia, which is the only region of Canada bordering the Pacific Ocean, is an important part of this system. The Provincial Emergency Program (PEP) must receive Watch and Warning messages from the West Coast/Alaska Tsunami Warning Center (WC/ATWC) and relay those messages, with refinements for Canadian coast and tidal conditions, to all sectors of the population at risk in the province (Rapatz and Murty, 1987). The initial tsunami warning is based on seismic information, in particular on the magnitude,  $M_w$ , of the respective submarine earthquake (the magnitude threshold value for tsunami warning is  $M_w = 7.5$  for distant Pacific earthquakes and  $M_w = 7.0$  for local earthquakes). However, sometimes even very strong earthquakes do not generate widespread destructive tsunamis, resulting in costly false alarms. For example, the false tsunami warning associated with the 1994 Shikotan Earthquake ( $M_w = 8.2$ ) resulted in lost productivity valued at a few million dollars for British Columbia. On the other hand, sometimes even relatively weak local earthquakes produce significant tsunami waves for the Pacific coast of North America capable of devastating communities in the near field (González *et al.*, 1995). Thus, a magnitude 5.2 earthquake in 1930 reportedly generated a 6 m wave in Santa Monica, California (Bernard, 1998). The coasts and underwater slopes of British Columbia contain significant amounts of unstable material, so submarine and subaerial landslides, slumps and rock falls and associated tsunamis are often the secondary effects of earthquakes (Evans, 2001; Rabinovich *et al.*, 2003). To reduce the impact of tsunamis for coastal areas, help prevent false alarms, and mitigate the tsunami hazard, it is important to establish a reliable network of deep-ocean and coastal tide gauges/tsunami recorders (Bernard, 1998). Such

gauges are also essential for estimation of resonant properties of local topography, constructing maps of tsunami risk along the coast (local tsunami-zoning), and issuing detailed wave height and wave arrival information for incoming waves (Mofjeld *et al.*, 1999, 2000).

Tide gauge measurements on the B.C. coast started in the 1890s. The earliest tide gauge on the outer (oceanic) coast was established at Clayoquot (now known as Tofino) on the west coast of Vancouver Island in 1905. This tide gauge has been in continuous operation since that time and provides the most comprehensive record of tsunami events on the B.C. coast (Wigen, 1983). Over the years the number of permanent gauging stations gradually increased, and a number of temporary stations were installed in support of hydrographic and oceanographic surveys. The 1960 Chile tsunami was observed at 17 B.C. stations (Rapatz and Murty, 1987). The 1964 Alaska tsunami was recorded at 12 stations; the largest waves (with trough-to-crest wave heights more than 5 m) were observed in Port Alberni (Wigen and White, 1964).

In the 1960s–1970s all tide gauges on the B.C. coast were analogue. Records of reasonably high quality were collected (Wigen, 1983), but with the exception of a very rudimentary automated warning system at Tofino, sea level records were not available for real-time analysis in response to potential tsunami events. Basic information could be obtained from gauge attendants by telephone or radio, but the record could only be analysed and digitised days or weeks after the event. The accuracy of these instruments was a few centimetres. In the 1980s the Canadian Hydrographic Service (CHS) began to operate both digital and analogue gauges at key stations on the B.C. coast. This gave the tsunami response team access to the data in real time by either telephone modem or by Meteor Burst communication. For the most part though, on-site data storage and throughput considerations limited the data sampling interval to 15 minutes.

The catastrophic tsunamis of the last decade initiated (1998) a major upgrade of the existing tsunami warning and Permanent Water Level Network (PWLN) stations on the B.C. coast. The new digital instruments were designed to continuously measure sea level variations with much higher precision than the earlier analogue gauges, and to store corresponding sea level samples every minute. During the period 1999–2001 long series of high quality 1-minute sea level data were collected and two weak tsunamis (the trans-Pacific Peru tsunami of June 23, 2001, and the local Queen Charlotte tsunami of October 12, 2001) were recorded.

The purpose of the present study is to use the records of these two tsunamis, together with background records obtained during both calm and storm weather conditions, to estimate the data quality of all stations and the efficiency of these stations for tsunami monitoring. Identification and separation of seismically generated tsunami waves and atmospherically generated seiche oscillations (“meteorological tsunamis”) is a key problem for CHS personal and an important scientific problem (Rabinovich and Monserrat, 1996; González *et al.*, 2001). Within this study,

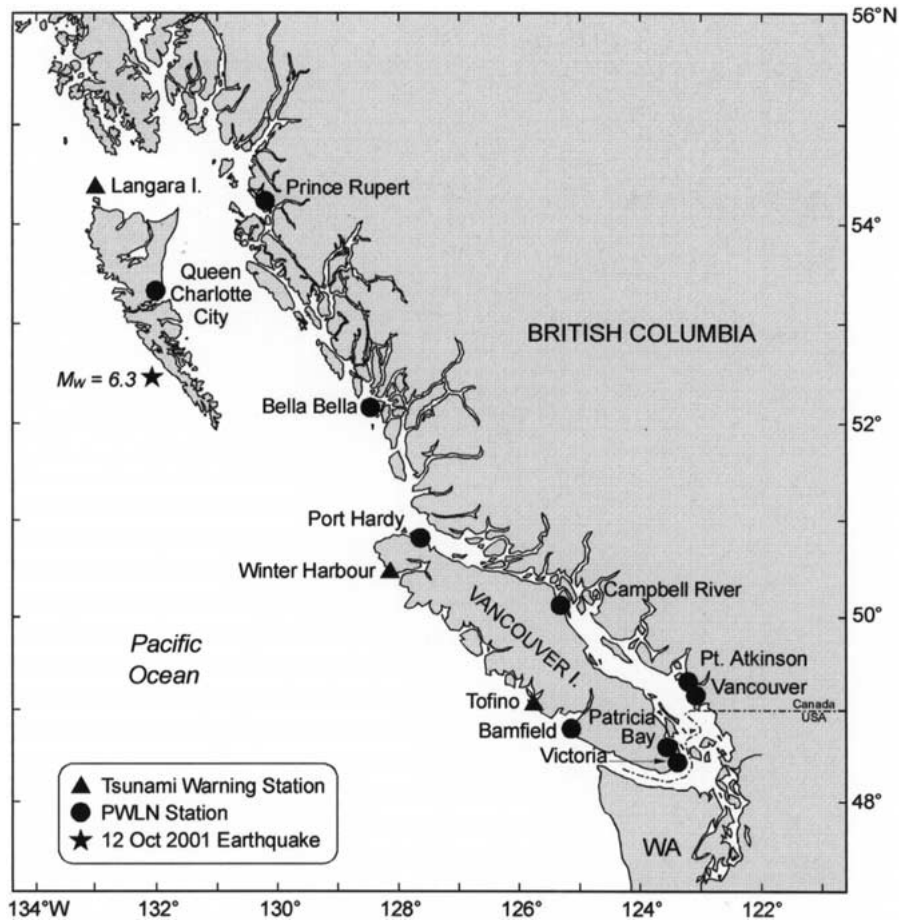


Figure 1. Location of tide gauges on the coast of British Columbia. Tsunami warning stations are marked by triangles, the other Permanent Water Level Network (PWLN) stations are indicated by circles. The epicenter of the October 12, 2001 Queen Charlotte earthquake ( $M_w = 6.3$ ) is indicated by a star.

we also examine the resonant characteristics of local topography and possible amplification of tsunami waves approaching the coast from the open ocean.

## 2. Upgraded Tsunami Warning System

The 1998 upgrade was undertaken to address major shortcomings of the earlier digital systems, and was fortunately driven to a large degree by government concerns about emergency response continuity in the year 2000. By 1999, 13 tide gauge stations were upgraded and operational (Figure 1). Three of these stations, located along the outer coast (Tofino, Winter Harbour, and Langara), were selected for use in tsunami warning.

The tsunami warning stations at Tofino and Winter Harbour have stilling wells, with float and counterweight mechanisms and dual gray-code (BEI) encoders. This measurement technique is used at all of the other tide gauge stations except Langara. Due to its exposed location the Langara tsunami warning station uses a bubbler system with a quartz crystal (Paroscientific) differential pressure sensor. Each of the three tsunami warning stations is equipped with RST 2000 Mobile Satellite (MSAT) packet data mobile earth terminals (MET). Should a tsunami event occur, a detection algorithm within the Sutron data logger would cause the MET to transmit an emergency message (Figure 2). The gauge computes the mean per minute change from the last three minutes of observations and compares this value with a threshold value (e.g. 16 mm/min at Tofino). If the threshold value is exceeded for three consecutive minutes, a tsunami alarm is generated. The algorithm has been designed to provide the lowest possible detection threshold without triggering false alarms due to ordinary atmospherically generated seiches. A host computer at the Institute of Ocean Sciences (IOS) receives the alarm message and automatically issues a pager call to alert response personnel to investigate the tsunami event. Data can then be requested by the Host computer and forwarded to the pager for ongoing analysis and response.

Under normal conditions the sea levels at every tsunami and PWLN station are sampled continuously and stored every minute. At all stations, except Langara, these data are then transited by telephone modem every three hours to the Host computer for storage. At Langara the gauge operation is checked daily and data backups are made monthly (to floppy disk) and mailed to the IOS. In normal operation, the MSAT communication mode (Figure 2) is not used, however, an 'event' will trigger its operation. The communication link can also be transferred to MSAT at any time by response personnel using the telephone modem, or during a brief time window every 15 minutes when the remote MSAT unit powers up to look for incoming messages (Figure 2).

The new hardware has been in operation since early 1999. During this period the data return has been in excess of 99% from the network, with most stations providing 100% data return. The present network is reliable, and the data it provides are accurate and timely. However, most of the tsunamis recorded on the B.C. coast have trough-to-crest heights less than 20 cm, and over the last 37 years none have had heights greater than 20 cm. When a potentially tsunamigenic earthquake occurs, the Alaska Tsunami Warning Center (ATWC) provides information on the location and magnitude of the event, as well as expected tsunami arrival times at various locations around the Pacific coast. Following these predicted arrival times emergency response personnel expect to begin receiving information on the observed/recorded tsunami. Response staff need to be able to quickly and accurately estimate the wave heights of arriving waves, determine if the measured signals are tsunami or merely atmospherically generated seiches, and assess the danger of the arriving waves for the coastal communities. That information must be quickly passed to the ATWC and to local emergency response personnel.

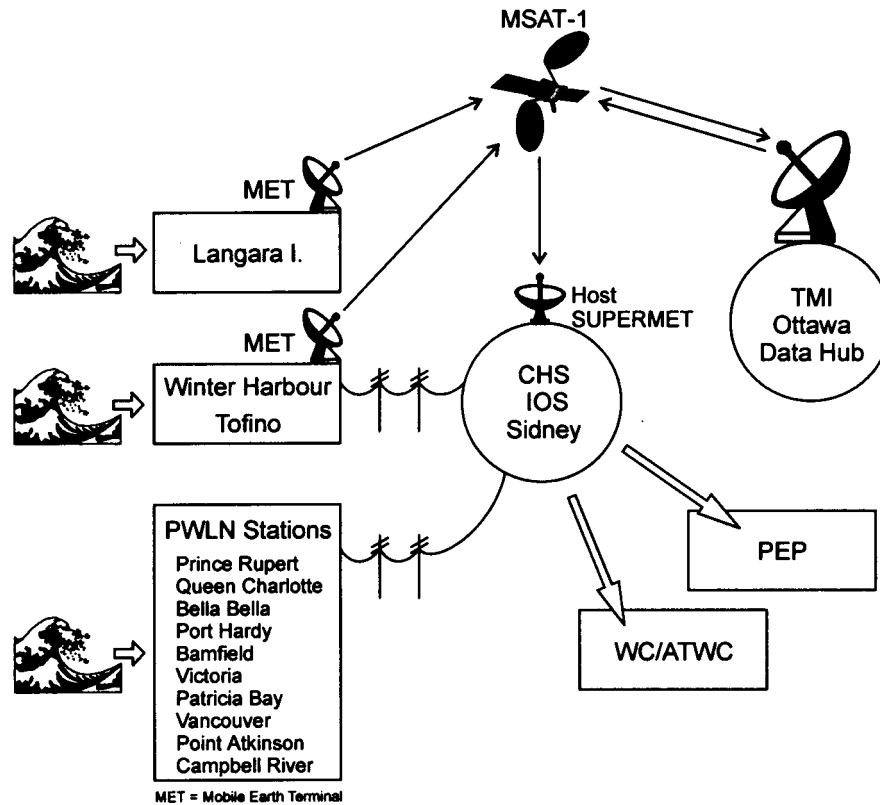


Figure 2. Present scheme of tsunami monitoring on the coast of British Columbia based on tsunami warning and PWLN stations.

Separation of real tsunami waves from atmospherically induced seiche oscillations is a key problem for the Tsunami Warning System and one of the main goals of the present study. At the same time, comparison of spectral characteristics of long waves caused by seismic and atmospheric sources is an important scientific problem, which can help in understanding the generation mechanisms of both types of processes (Rabinovich, 1997; González *et al.*, 2001).

### 3. October 2000 Storm and Background Longwave Oscillations

To examine resonant topographic characteristics (frequency response) of the B.C. tide gauge stations and reaction of sea level at these stations to atmospheric disturbances, we used simultaneous nine-day records at all stations shown in Figure 1 except Langara. The selected segment, October 23–October 31, 2000, included a major storm, which struck the coast of British Columbia on October 27–29, 2000. Unfortunately, because of problems with the on-site data backups, the Langara tide

gauge record is not available for this period and another segment of data (October 28–November 5, 1999) was analysed instead for this station.

### 3.1. GENERAL DESCRIPTION

The extent of the strong storm of October 27–29, 2000, is vividly displayed in the satellite image in Figure 3. The center of the cyclone had a surface barometric pressure of 960 mBar, more than 50 mBar below the annual mean atmospheric pressure for the British Columbia coast. Winds exceeding 30 m/s were observed when the cyclone crossed the west coast of Vancouver Island. All tide gauge stations (marked in Figure 3 by circles) recorded a significant increase of sea level along the coast, which was 70–100 cm above the predicted tidal levels. Large seiche oscillations were also recorded at a number of stations during the storm passage.

Tidal oscillations (large tides) on the B.C. coast range from 3.4 m in the south (Victoria) to 7.8 m in the north (Queen Charlotte City). With these large tide ranges even a major event, such as the October 27–29 storm surge, is not readily apparent in the records. Table I shows total variances of sea level oscillations at all stations, variances of the predicted tides, and variances of the residual (non-tidal) oscillations (after subtraction of 38 predicted tidal constituents). The table shows that tides are responsible for about 98% of the total energy of sea level oscillations. The absolute energy of the residual oscillations is similar for different stations, and is mainly related to the storm surge; the energy of the relatively high-frequency oscillations in the tsunami frequency band (0.01–0.5 Hz) is different for different sites.

The predominance of tidal oscillations makes direct examination of the non-tidal signal (in particular, weak tsunamis) difficult. However, the high quality of tidal prediction enables us to remove tides from the original records without distorting the non-tidal oscillations (Subbotina *et al.*, 2001). Figure 4 shows the sea level residuals for the period October 23–31, 2000. A large storm surge with a peak value on October 28 is evident in all records. The maximum heights (more than 1.0 m) were observed at Queen Charlotte City, Winter Harbour and Tofino. What is of interest to us, are the high-frequency oscillations accompanying this surge. These oscillations have approximately the same frequencies as seismically generated tsunami waves and look very similar to the latter, so following Defant (1961), Rabinovich and Monserrat (1996) and González *et al.* (2001) we will use the term “meteorological tsunamis” to identify them. A high passed Kaiser-Bessel filter (Emery and Thomson, 2001) with 3-hour window was applied to the data to display these oscillations (Figure 5). The maximum seiche oscillations were observed on October 28 and 29 at Winter Harbour, Tofino and Bamfield, the three stations along the west coast of Vancouver Island. Significant waves were also observed at Victoria, Queen Charlotte City and Port Hardy, however, the duration of the wave trains was only 20–24 hours, compared with 48 hours for stations along the west coast. Anomalous regular oscillations with wave heights of about 15 cm

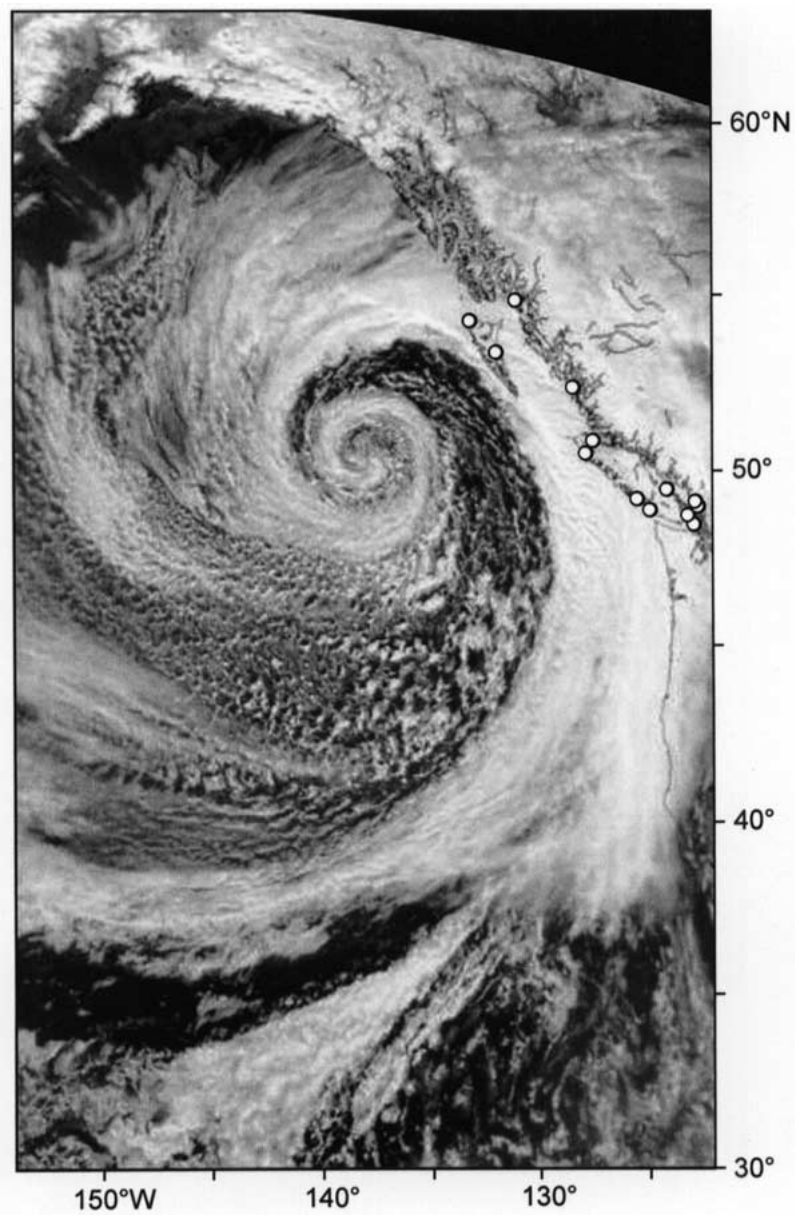


*Figure 3.* Visual satellite image of the strong cyclone of October 27, 2000 captured by the SeaWiFS satellite as it passed over the northeast Pacific. Positions of the tide gauges on the coast of British Columbia are marked by the circles.



*Table I.* Variances of sea level oscillations at various tide gauge stations on the coast of British Columbia for the period October 23–31, 2000. Symbol ▲ marks tsunami warning stations

Station	Variance				
	Total (m <sup>2</sup> )	Tidal		Residual	
		(m <sup>2</sup> )	(%)	(m <sup>2</sup> )	(%)
Prince Rupert	3.415	3.397	99.47	0.018	0.53
Langara* ▲	1.036	1.028	99.23	0.008	0.77
Queen Charlotte City	3.572	3.553	99.47	0.019	0.53
Bella Bella	1.535	1.520	99.02	0.015	0.98
Port Hardy	1.618	1.605	99.20	0.013	0.80
Winter Harbour ▲	0.929	0.903	97.20	0.026	2.80
Tofino ▲	0.857	0.828	96.62	0.029	3.38
Bamfield	0.810	0.787	97.16	0.023	2.84
Victoria	0.293	0.271	92.49	0.022	7.51
Patricia Bay	0.508	0.486	95.67	0.022	4.33
Vancouver	1.008	0.984	97.62	0.024	2.38
Point Atkinson	0.980	0.954	97.35	0.026	2.65
Campbell River	0.760	0.736	96.84	0.024	3.16
Mean	1.332	1.312	98.50	0.020	1.50

\*Variance estimates for the station Langara are obtained for the period October 28–November 5, 1999.

were recorded in Campbell River. The periodicity of the corresponding trains was about 25 hours and these oscillations were associated with low tides. Apparently they are related to some local effect. We have not used this station in the following analysis.

### 3.2. SPECTRAL ANALYSIS

To examine the spectral properties of longwave oscillations at each station we divided the 9-day data records into two parts: The period from October 23 to October 26, 2000, preceding the storm surge event, was identified as “normal” and selected for analysis of background signals; the period from 12:00 (PST) on October 27 to October 30, 2000 (the “storm period”) was chosen for analysis of storm oscillations. For the purpose of the Fast Fourier Transform (FFT) the lengths of both selected pieces (“normal” and “storm”) were 4096 min (~ 68.3 hr). The same division was made for Langara, except that the selected pieces were from October 28 to October 31, 1999 (“normal”) and from November 1 to November 4, 1999 (“storm”). To improve the spectral estimates, we used a Kaiser-Bessel spectral window (Emery and Thomson, 2001) with half-window overlaps prior to the Fourier transform. The length of the window was chosen to be 512 min,

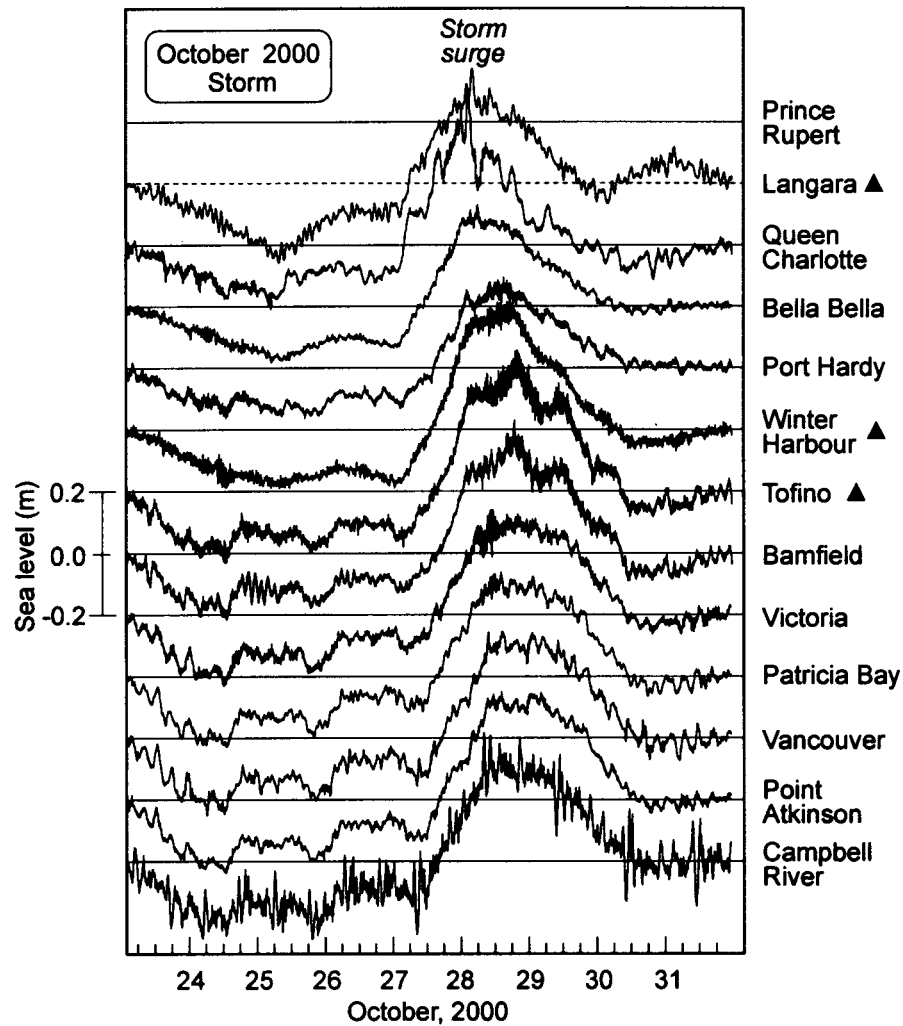


Figure 4. Residual (non-tidal) records of the tide gauges on the B.C. coast from October 23 to October 31, 2000. Symbol ▲ marks tsunami warning stations. Strong storm surge of October 27–29 is clearly seen in the records.

yielding degree of freedom  $\nu = 30$ . Figure 6 shows the results of the analysis for 12 stations of the B.C. coast.

In general, the spectra are “red”, with spectral energy rolling off at increasing frequency as  $\omega^{-2}$  (Figure 6). This is typical for longwave spectra (cf. Aida *et al.*, 1972; Kulikov *et al.*, 1983; Rabinovich, 1993, 1997). The longwave spectra for the Langara station (both “normal” and “storm”), however, are exceptional in that: at high frequencies ( $> 0.02$  Hz) they resemble “white noise”. Similar results were obtained for other 1999–2001 segments of data from this station, suggesting either poor instrument quality (insufficient accuracy) or aliasing due to the strong

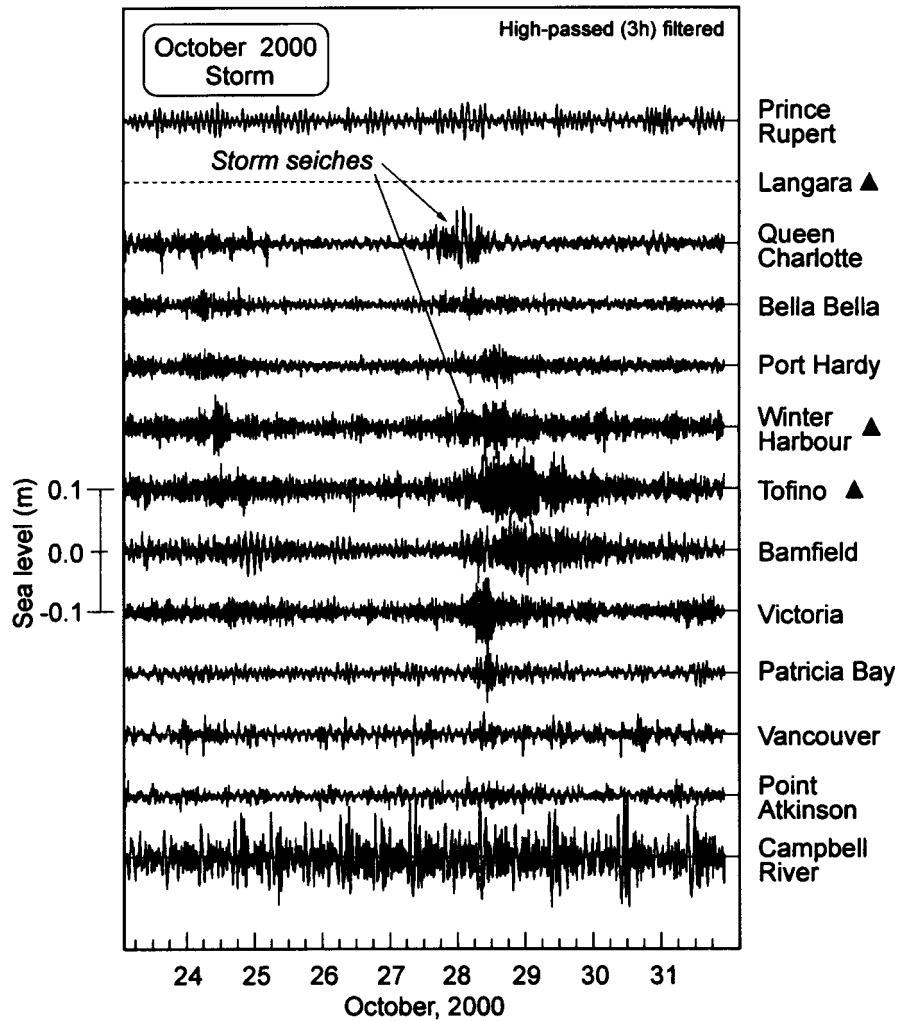


Figure 5. The same as in Figure 4 but high-passed with 3-hour Kaiser-Bessel window.

influence of wind waves/swell. The Langara station is at a very rugged and exposed location and is known to have operational problems that need to be addressed.

The spectral maxima and minima at each station were different (the resonant periods of the main spectral peaks are identified in Figure 6), indicating significant local topographic effects. All stations except Langara, responded well at all frequencies; the resonant peaks are almost the same for the two states (“normal” and “storm”). This result is in good agreement with the well known fact that periods of extreme events (e.g. tsunamis or meteo-tsunamis) are mainly related to resonant properties of local topography, rather than to characteristics of the source, and are almost the same as those of background oscillations for the same sites (Honda *et al.*, 1908; Miller, 1972; Rabinovich and Monserrat, 1996). For all stations the

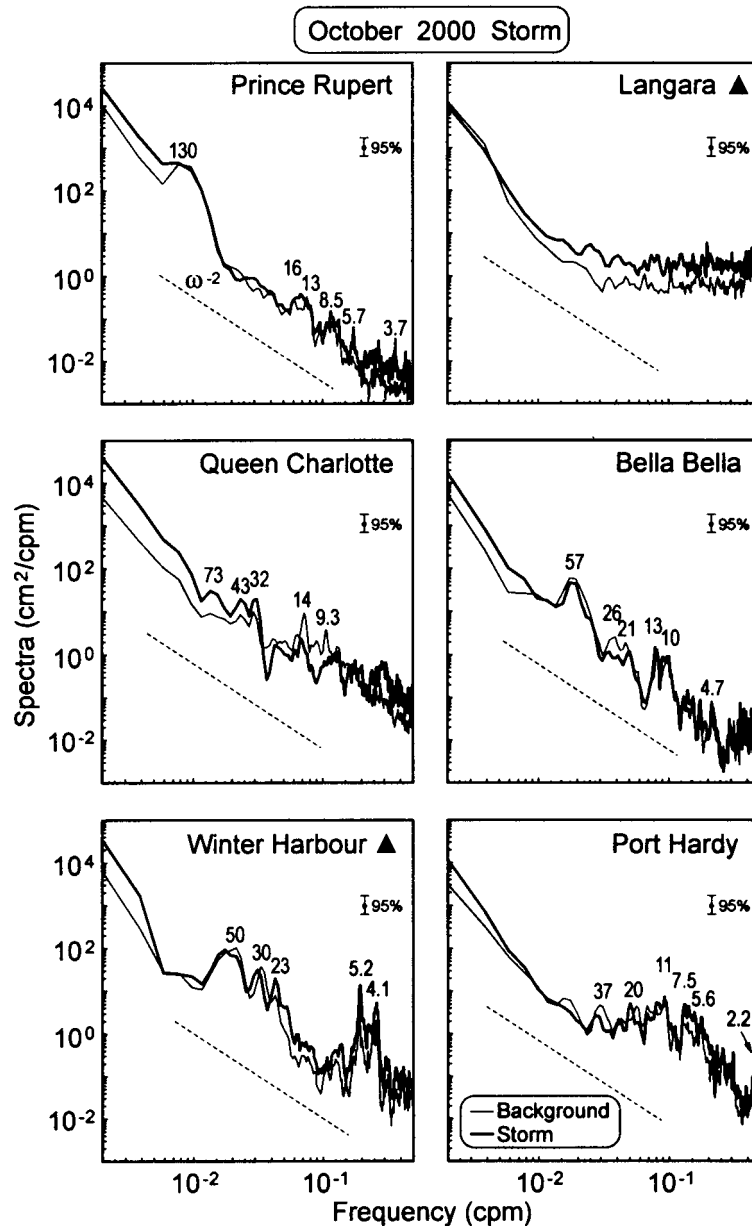


Figure 6. Spectra of background and storm sea-level oscillations on the B.C. coast (October 23–31, 2000). Periods (in min) of the main spectral peaks are indicated.

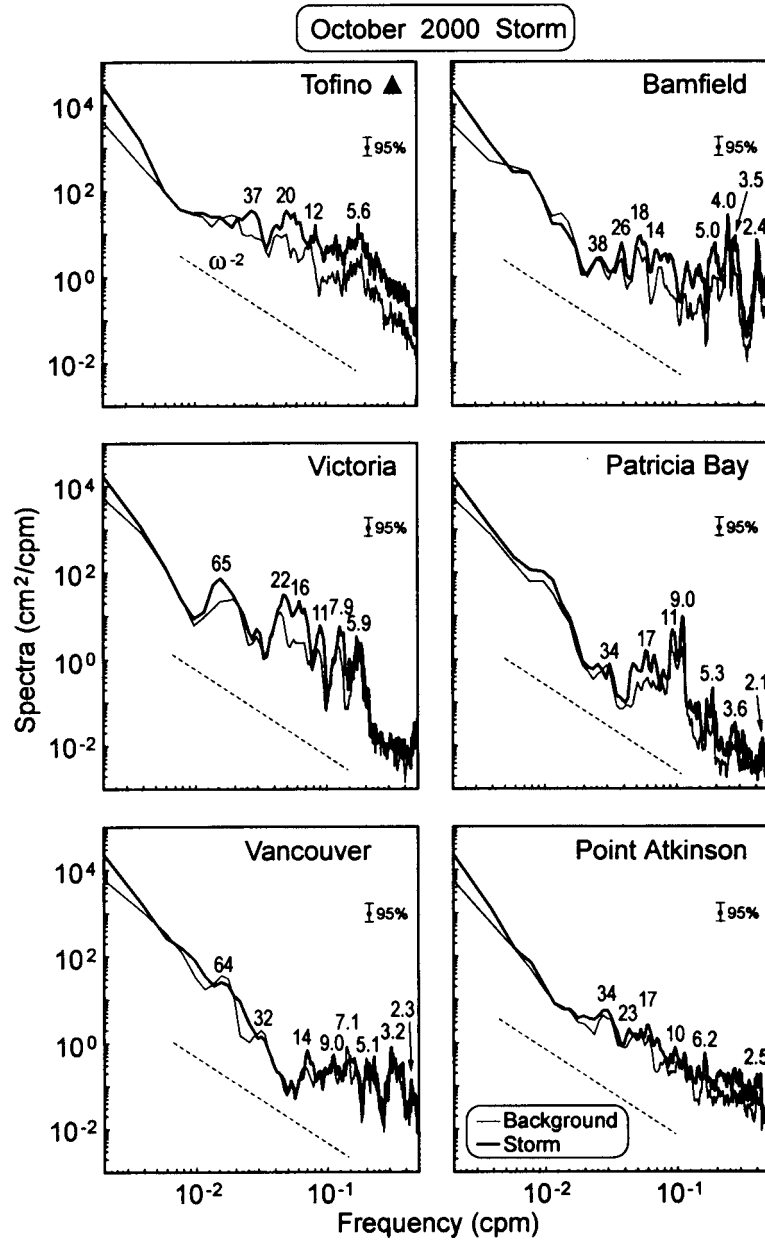


Figure 6. Continued.

spectra shows much more energy during the storm event than during “normal” weather.

### 3.3. TOPOGRAPHIC ADMITTANCE

Long waves (in particular, tsunamis) arriving from the open ocean are strongly affected by local topography and bathymetry, such as continental shelves and associated bays and harbours. These waves may amplify significantly near the coast due to local resonant effects. For example, the destructive tsunami waves observed on the B.C. coast at Port Alberni after the 1964 Alaska earthquake were caused by a strong resonance in Alberni Inlet (Murty, 1977, 1992). That is why estimation of eigen periods of bays, inlets and harbours is a key part of long-term tsunami forecast (Mofjeld *et al.*, 1999, 2000). The customary method of such estimation is numerical modelling (Raichlen *et al.*, 1983; Mofjeld *et al.*, 1999). Unfortunately, this method is very laborious and needs detailed bathymetry. However, some simple estimates of local topographic response may be obtained directly from sea level spectra without complicated numerical computations.

Consider the resonant characteristics of local topography for different sites. Linear sea level oscillations  $\zeta(t)$  recorded at time  $t$  by a tide gauge near the coast may be described as a convolution of the source  $Z(t)$  and the topographic response function  $w(t)$

$$\zeta(t) = \int_0^{\infty} w(\tau)Z(t - \tau) d\tau. \quad (1)$$

In the spectral domain, (1) may be expressed in the form

$$S(\omega) = W(\omega)E(\omega), \quad (2)$$

where  $\omega$  is the angular frequency,  $S(\omega)$  is the spectrum of sea levels,  $W(\omega) = H^2(\omega)$ ,  $H(\omega)$  is the admittance function describing the linear topographic transformation of long waves approaching the coast, and  $E(\omega)$  is the source spectrum. Suggesting that the observed spectra may be presented in the form (2), we thereby assume that all individual peculiarities of the observed spectrum  $S_j(\omega)$  at  $j$ th site are related to the individual topographic function  $H_j(\omega)$ , while all general properties of this spectrum are associated with the source (certainly if the source is the same for different stations) (see Rabinovich, 1997 for details). For ordinary background oscillations  $E(\omega) = S_0(\omega)$ , where  $S_0(\omega)$  is the longwave spectrum in the open ocean.

Long-term bottom pressure measurements in the various regions of the Pacific Ocean (Kulikov *et al.*, 1983; Filloux *et al.*, 1991) have demonstrated that in the deep open ocean function  $S_0(\omega)$  is smooth and monotonic and almost universal. It may be roughly described as

$$S_0(\omega) = A\omega^{-2}, \quad (3)$$

where  $A = 10^{-3}\text{--}10^{-4} \text{ cm}^2\cdot\text{Hz}$  is a constant slightly dependent on atmospheric activity and individual properties of the basin (see also Aida *et al.*, 1972). As it follows from (2) and (3), function  $H_j(\omega)$  for  $j$ th station may be expressed as

$$H_j(\omega) = \left[ \frac{S_b^j(\omega)}{S_0(\omega)} \right]^{1/2} = \omega \left[ \frac{S_b^j(\omega)}{A} \right]^{1/2}, \quad (4)$$

where  $S_b^j(\omega)$  is the background spectrum observed at  $j$ th station. Topographic admittance function  $H_j(\omega)$  is the characteristic of each station describing frequency transformation of the open ocean signal into a signal observed at this station.

We applied expression (4) to compute  $H_j(\omega)$  for twelve stations on the B.C. coast. For this purpose we used the observed background spectra shown in Figure 6 and assumed that  $A = 10^{-3} \text{ cm}^2\cdot\text{Hz}$ . The results presented in Figure 7 demonstrate individual resonant properties of the various sites. In fact, function  $H_j(\omega)$  describes integral effect of topography on arriving waves; without special numerical experiments we cannot separate the effect of different topographic features and explain the exact nature of the resonant peaks in  $H_j(\omega)$ . However, we may suppose that relatively high-frequency peaks with periods 2–15 min are related to eigen oscillations in local bays and harbours, while low-frequency peaks (20–130 min) are associated with the standing oscillations in larger bays, inlets and straits, as well as with the shelf resonance.

As shown in the plots presented in Figure 7, some stations (Bamfield, Tofino, Winter Harbour, Victoria, Port Hardy) have evident resonant properties; at these stations long waves arriving from the open ocean may amplify 10–15 times. In contrast, in Prince Rupert the waves from the open ocean with periods less than 2 hours (i.e. at tsunami frequencies) do not amplify and even become weaker near the coast. Stations Bella Bella and Point Atkinson also have vague resonant properties. The topographic function for Langara is “abnormal”, presumably more because of instrumental problems than of any real local topographic response. Taking into account that tsunami waves approaching the coast amplify normally in the same way as ordinary background waves, we may expect significant tsunamis in Tofino, Bamfield, and Winter Harbour, but not at Prince Rupert, Bella Bella or Point Atkinson.

#### 4. Peru Tsunami of June 23, 2001

On June 23, 2001 a magnitude  $M_w = 8.4$  earthquake occurred at 20:33 UTC (12:33 PST) off the coast of southern Peru. This earthquake generated a widespread tsunami, which was recorded in several places along the Pacific coast, including Australia and Japan. The possibility of such a catastrophic earthquake and tsunami, which claimed at least 23 lives, was predicted by Rabinovich *et al.* (2001) who four months before the event wrote: “A region between  $15^\circ$  S and  $24^\circ$  S, straddling the Peru/Chile border, lies a ‘seismic gap’ which has not experienced an earthquake

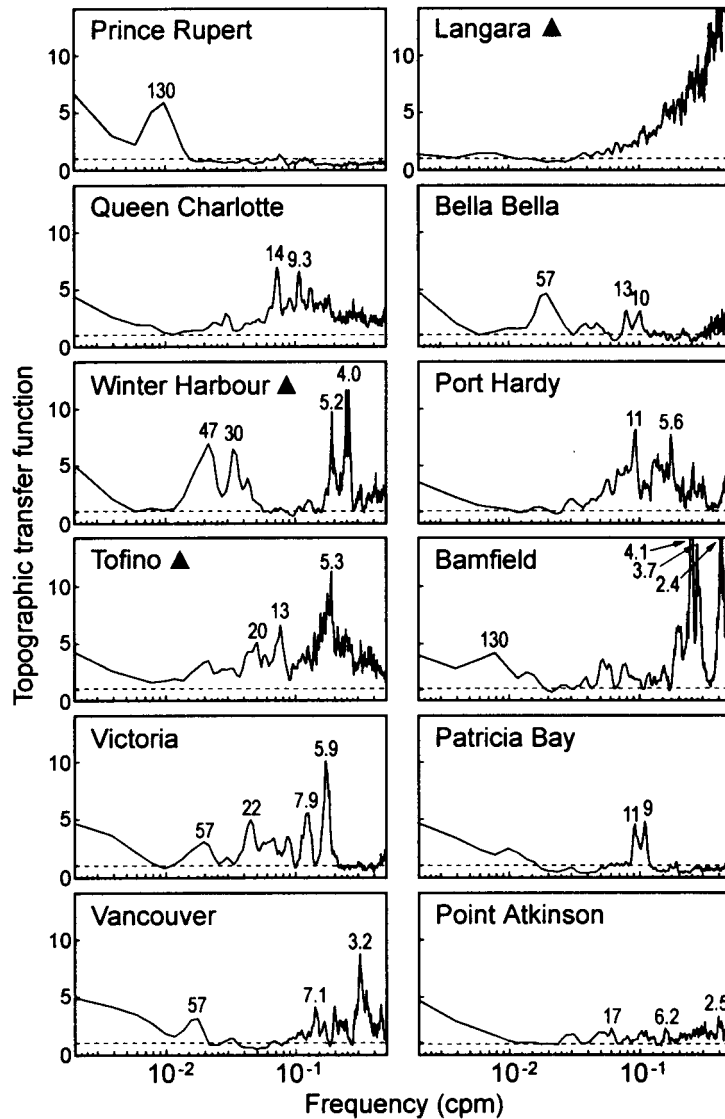


Figure 7. Topographic transfer (admittance) functions for 12 stations on the B.C. coast. Periods (in min) of the main peaks are indicated.

since 1877. Thus, it has high potential for a major earthquake of magnitude greater than 8.0. . . . By crude estimates, tsunamis with wave heights of about 16 m . . . are likely to occur in the near future". The actual tsunami run-up estimated by the International Tsunami Survey Team, in the Camana area, Peru, was more than 9 m (Okal *et al.*, 2001). The preliminary modelling of this event (Geist *et al.*, 2001), as well as the direct observations of sea levels on the coast of New Zealand (Goring, 2002), show that most of the energy of the 2001 Peru tsunami went southwestward,



i.e. in the direction of New Zealand and Australia. However, a certain portion of the energy also went poleward (to the north and south) along the American coast.

Immediately after the earthquake (at 12:33 PST), an information bulletin was issued by the WC/ATWC and the Canadian Hydrographic Service tsunami response personnel were in communication with the Provincial Emergency Program by 13:40 PST. Once the exact location of the earthquake was known, there was little expectation that a significant tsunami wave would strike the B.C. coast located about 10,000 km from the source area. Of the 98 earthquake events in the Chile–Peru area inspected by Wigen (1983) for the period 1906 to 1980 only two produced a measurable ( $> 6$  cm) tsunami at Tofino (1922 and 1960). Nevertheless, the stations were checked to ensure that all instruments were fully operational for the possible tsunami. No tsunamis along the B.C. coast were witnessed directly during the event. However, further analysis of the tide gauge records (after subtraction of predicted tides) showed that this tsunami was recorded by several instruments, including all three tsunami stations (Winter Harbour, Tofino, and Langara).

Figure 8 presents the residual signal for 12 stations on the B.C. coast. The vertical line marked E indicates the time of the earthquake. The expected tsunami arrival times (ETA), as provided by WC/ATWC, are shown for Tofino and Langara. The tsunami event is clearly evident in the records of the stations on the west coast of Vancouver Island (Tofino, Winter Harbour, and Bamfield). As demonstrated in the previous section, these stations have striking resonant properties for waves in the tsunami frequency band (see Figure 7). The tsunami signal can be also identified in the plots of five other stations (Langara, Victoria, Port Hardy, Queen Charlotte City, and Bella Bella) mainly located on the Pacific coast, or along the adjoining straits. In contrast, stations Patricia Bay, Vancouver, and Point Atkinson located in or near the inland part of the Strait of Georgia (see Figure 1) did not record this tsunami. It also was not recorded at Prince Rupert, the station with weak topography response at tsunami frequencies (Figure 7).

To better display the tsunami records, we used a high-passed filter. Figure 9 shows these records for eight selected stations on the B.C. coast for the same period of time as in Figure 8. Estimated maximum tsunami wave heights (trough-to-crest) for these stations were the following: 9.5 cm (Langara), 3.7 cm (Queen Charlotte), 6.7 cm (Bella Bella), 5.4 cm (Port Hardy), 12.9 cm (Winter Harbour), 15.1 cm (Tofino), 9.7 cm (Bamfield), and 7.4 cm (Victoria).

The records presented in Figure 8 have certain specific features distinguishing them from the typical tsunami records:

1. Despite an obvious increase of long-wave energy during the event, the precise arrival time of the first wave and its polarity (positive or negative) are not clear in the records. It appears that tsunami-driven seiches simply augmented the existing atmospherically generated seiches (eigen oscillations) in the corresponding bays, inlets or harbours.

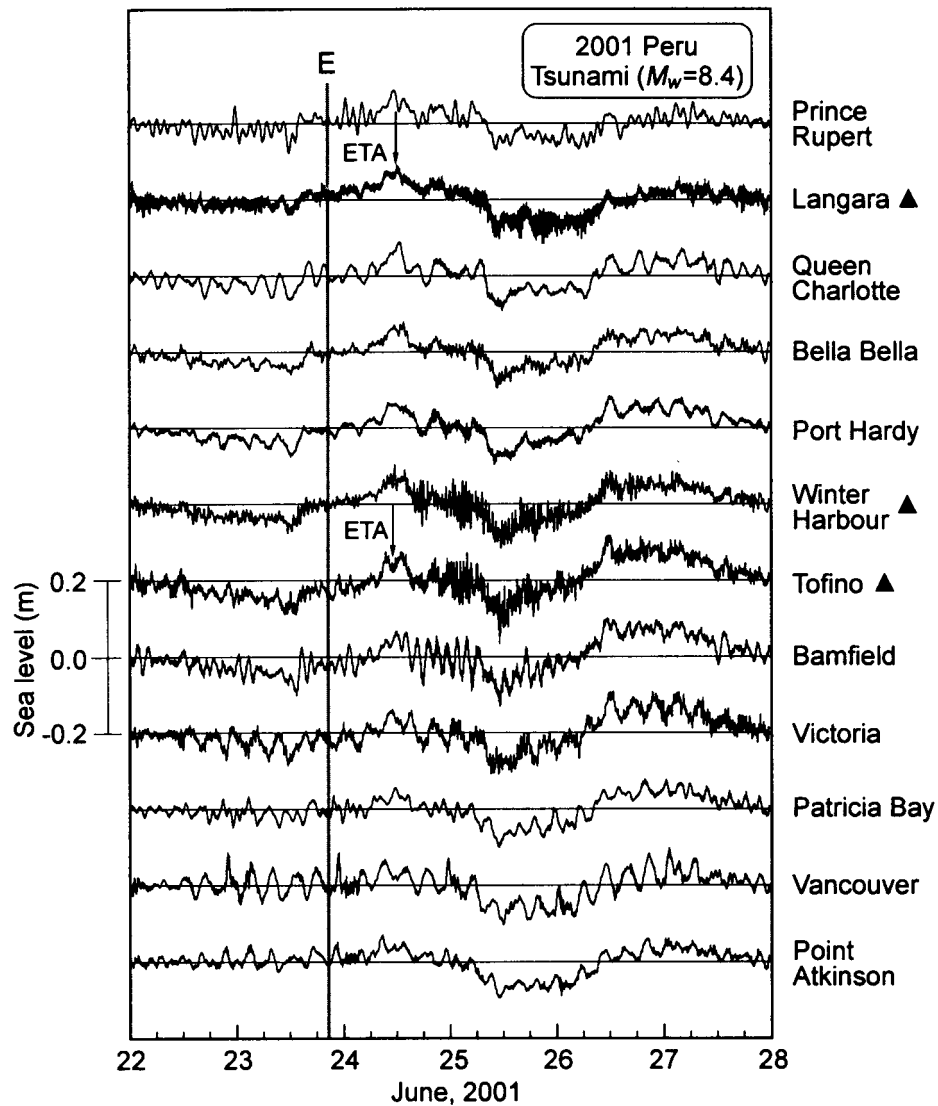


Figure 8. Residual (non-tidal) records of the tide gauges on the B.C. coast for June 22–27, 2001. Symbol ▲ marks tsunami warning stations. The vertical line (E) indicates the moment of the Peru Earthquake ( $M_w = 8.4$ ). Arrows mark estimated tsunami arrival time (ETA) to the corresponding stations.

2. Several well-defined packets of long waves are apparent in the records. These packets, recorded at different stations, closely resemble each other.
3. Maximum tsunami wave heights are mainly associated with the second or third packet; this means that these heights were measured about 1.5–2.0 days after the main shock, or about 1.0–1.5 days after the expected tsunami arrival time (ETA).

4. A significant increase of wave energy (compared with normal background noise) during the tsunami event was observed to persist for more than 4 days. Such prolonged “ringing” could be explained only by persistent incoming wave energy.

The above features suggest that the tsunami waves measured near the coast of British Columbia are mainly *edge waves*, which propagated along the continent coast to the observational sites from the source region. These waves are characterized by energy trapping over the shelf and much slower propagation speeds than *non-trapped (leaky) waves*. Miller *et al.* (1962) found that after the 1960 Chilean Earthquake energetic tsunami waves, having the form of trapped edge waves, had propagated along the South and North American coasts for more than a week.

For a semi-infinite sloping beach,  $h(x) = x \tan \beta$ , where  $h$  is the depth,  $x$  is the offshore coordinate, and  $\beta$  is the slope angle, the dispersion relation for edge waves is (LeBlond and Mysak, 1977):

$$\omega^2 = (2n + 1)gk \tan \beta, \quad n = 0, 1, 2, \dots, \quad (5)$$

where  $\omega = 2\pi/T$  is the angular frequency,  $T$  is the wave period,  $g$  is the acceleration due to gravity,  $k$  is the wave number, and  $n$  is the mode number. The phase speed of  $n$ th mode of edge waves is

$$c_n = \frac{\omega_n}{k} = (2n + 1) \frac{g}{\omega_n} \tan \beta = (2n + 1) \frac{gT_n}{2\pi} \tan \beta. \quad (6)$$

Thus, these waves are strongly dispersive with phase speed increasing with period and with mode number.

The ETA time computed by WC/ATWC from the June 23, 2001 Peru earthquake source area to Tofino is 14:43 PST, and to Langara 15:20 PST (Figures 8 and 9). This time corresponds to long non-dispersive leaky waves propagating in the deep ocean. Edge waves propagate much slower. For example, for  $\tan \beta = 0.02$  and period  $T = 20$  min, the fundamental mode ( $n = 0$ ) has phase speed  $c_0 \approx 140$  km/hr and needs about 3 days to travel from the source area to the B.C. coast. However, the same edge mode but with period  $T = 30$  min will arrive in 2 days, while the 20-min first mode ( $n = 1$ ) will come in 1 day. So, because of all these dispersive effects and interaction of the arriving waves with local resonant topographic features, the measured waves represent a complicated mixture of various oscillations, as we see in the observed records (Figure 9).

González *et al.* (1995), who analysed the 1992 Cape Mendocino tsunami, which occurred near the coast of northern California, found that on the Oregon and California coast (i.e. relatively close to the source area) the tsunami consisted of both non-trapped leaky waves and trapped edge waves. The former were responsible for the *first wave arrival* and the latter determined the *maximum wave arrival*. The reason for this difference is that the edge waves, bound to the shallow-water shelf, propagate along the coast providing energy conservation in this zone and slow

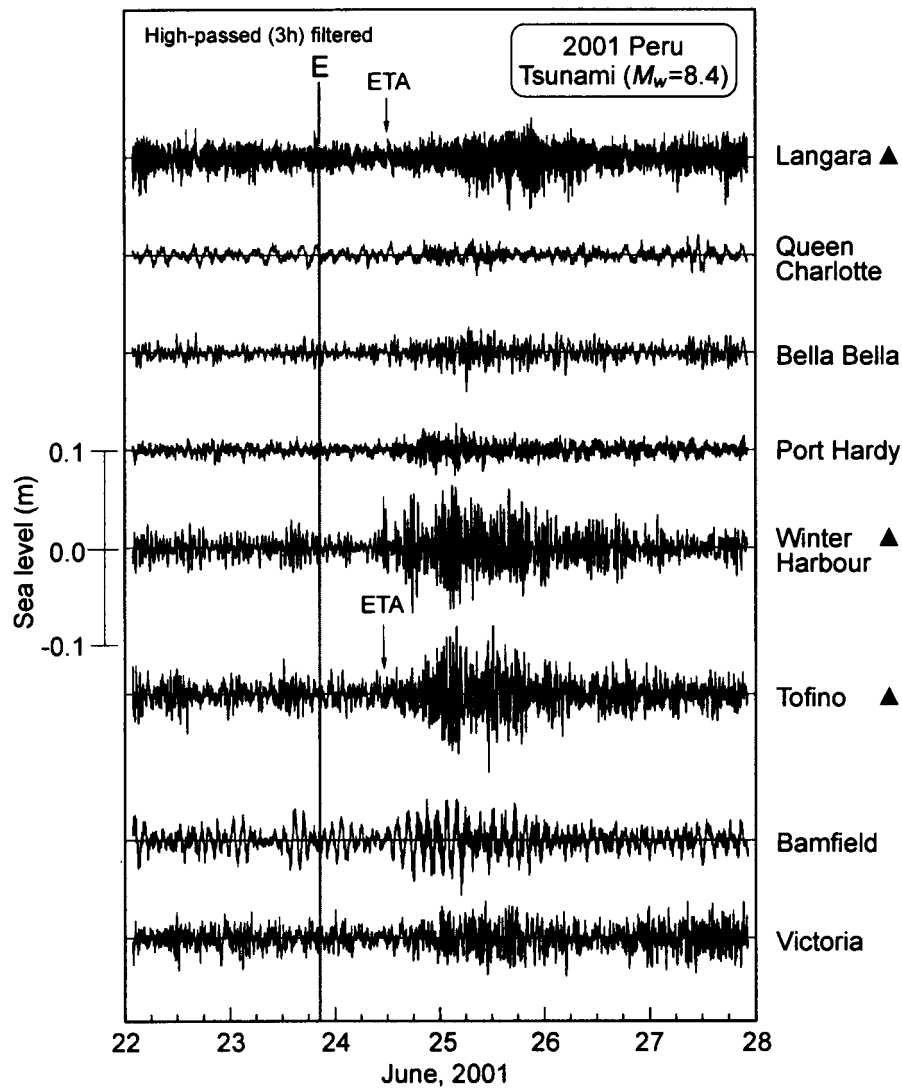


Figure 9. The same as in Figure 8 but after high-passed with 3-hour Kaiser-Bessel window and only for 8 stations.

wave height decay. In contrast, leaky waves spreading into the deep ocean have much higher phase speeds, however their heights decrease faster (roughly as the square root of the off-source distance). So, the dominance of edge waves for sites located on the same coast but far away from the source area (about 10,000 km for the examined event) is expected.

The spectral analysis technique used for the October 2000 storm event was also applied to examine the June 23, 2001 tsunami. The 8-day data records were divided into two parts: “pre-tsunami” (June 20–23) preceding the tsunami event,

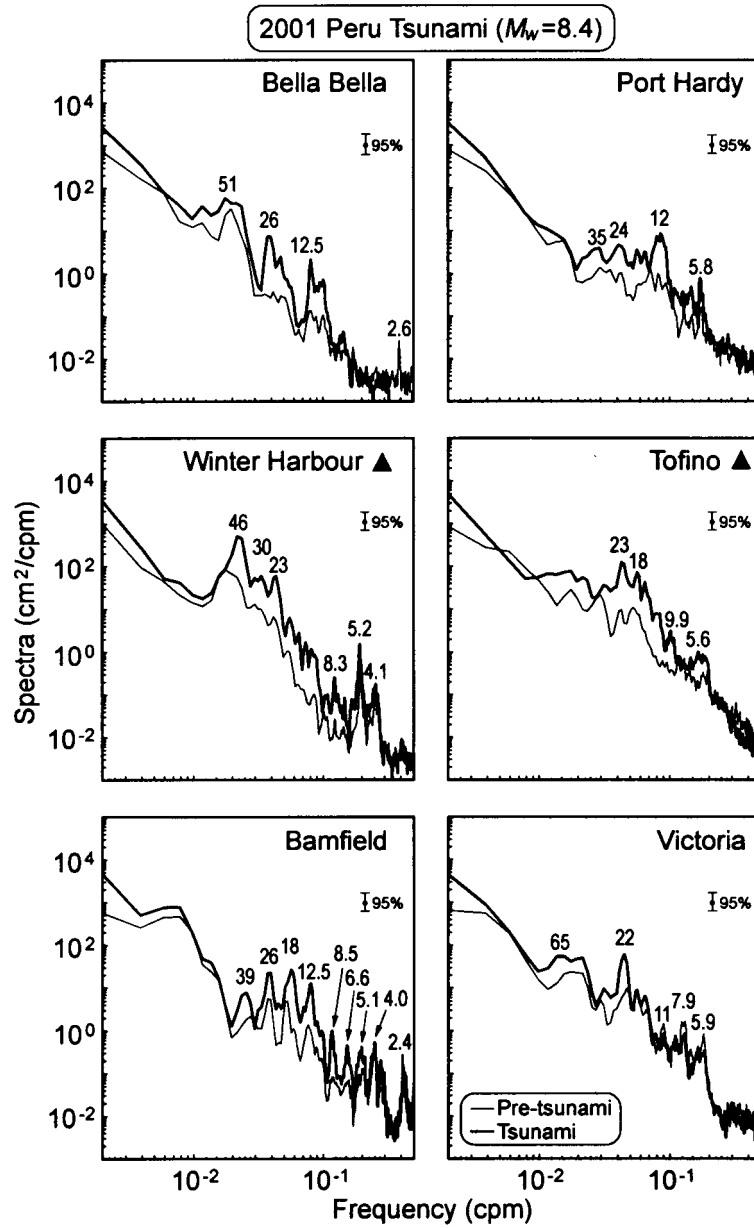


Figure 10. Spectra of pre-tsunami (background) and tsunami oscillations on the B.C. coast (June 22–27, 2001). Periods (in min) of the main spectral peaks are indicated.

and “tsunami” (June 24–27). Figure 10 shows the results of this analysis for six stations: Bella Bella, Port Hardy, Winter Harbour, Tofino, Bamfield, and Victoria. The results were comparable to those obtained for the October 2000 storm. In general, the difference between the background response and the event response was greater for the Peru tsunami than for the October storm. For both events almost the same spectral peaks were visible in the signal (compare Figures 6 and 10). Most of these peaks are associated with the respective peaks in the topographic admittance function of the corresponding stations (see Figure 7). The only exception was the tsunami station at Langara Island where the analysis indicated a poor response at periods less than 20–30 minutes.

### 5. October 12, 2001 Queen Charlotte Tsunami

On October 12, 2001 an earthquake with a magnitude  $M_w = 6.3$  (G. Rogers, Pacific Geoscience Centre, Sidney, B.C., Pers. Com.) occurred on the continental slope of the Queen Charlotte Islands (Figure 1). Surprisingly, this moderate underwater earthquake generated a tsunami, which was recorded by four tide gauges on the coast of Vancouver Island (Figure 11). Maximum tsunami wave heights at these stations were: 14.5 cm (Port Hardy), 22.7 cm (Winter Harbour), 18.2 cm (Tofino), and 11.3 cm (Bamfield). These heights exceed those for the June 23, 2001 Peru tsunami. Unfortunately, the Langara tsunami station was not in operation during this event, and at the other stations, including nearby stations Queen Charlotte, Bella Bella, and Prince Rupert, this tsunami was not recorded, probably because of coastal sheltering and spatial decay. The duration of “ringing” at these four stations was much shorter than for the Peru tsunami, lasting only 6–8 hours (Figure 11). To all appearances, this was a local tsunami, manifested within the bounds of coastal British Columbia.

We selected 8-hour segments to define “tsunami” spectra and 4-day record segments preceding the tsunami to define “background” spectra. The results of this analysis (not shown) are quite similar to those obtained for the October 2000 storm and for the June 2001 Peru tsunami.

### 6. Discussion

The key problem of our study is the difference in sea level response to tsunamis and atmospherically generated waves (meteorological tsunamis). González *et al.* (2001) write that “it is not possible to elucidate the source mechanism of the seiche excitations only by inspecting or analysing the sea level records”. Their conclusion is based on a statement by Rabinovich and Monserrat (1996) who, after studying catastrophic atmospherically generated “rissaga” waves on the coast of the Balearic Islands, concluded that “there are no differences between ‘meteorological’ or ‘seismic’ tsunamis with regard to their transformation in the coastal areas or their amplification in bays or harbours”. That is why González *et al.*

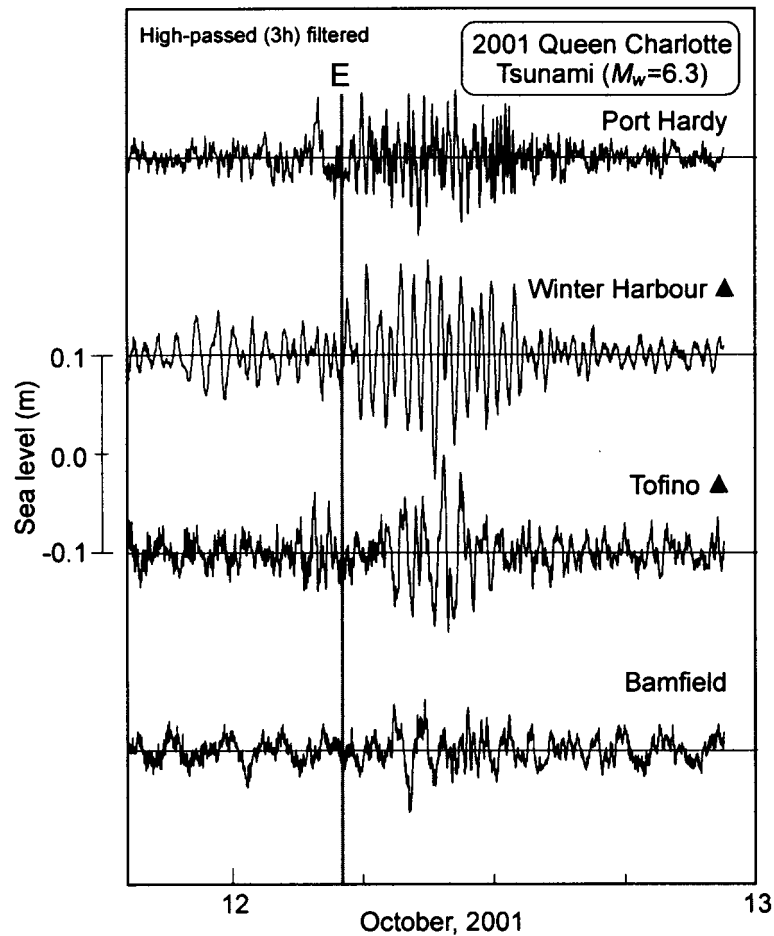


Figure 11. High-passed (with 3-hour Kaiser-Bessel window) records of the October 12, 2001 Queen Charlotte tsunami at four stations located on the coast of Vancouver Island. The vertical line (E) indicates the moment of the earthquake ( $M_w = 6.3$ ).

(2001) used computed travel times from the seismic and meteorological sources to the observation sites to explain the nature of high-amplitude seiches recorded in Manzanillo and Cabo San Lucas (Pacific coast of Mexico).

The B.C. tide gauge records of storm seiches (Figure 5) and tsunami seiches (Figure 9) look very similar, so it is unclear whether the source differences could be detected from analysis of tide gauge data alone without additional information on seismic or meteorological events. However, strong visible similarity of tsunamis and meteo-tsunamis are related to the same resonance influence of the local topography (Figure 7) and does not mean that their sources are similar. In fact, it is particular properties of the sources that can be used to distinguish between these two phenomena.

Rabinovich (1997) and Monserrat *et al.* (1998) suggested a simple approach to analyse tsunamis/meteo-tsunamis and to reconstruct their spectral source characteristics. The general idea is that by comparative analysis of the event and background spectra we can separate the source and topography effects. Eliminating the influence of topography and restoring the source, we can identify these phenomena and gain insight into their nature. Due to the absence of appropriate observational data, Rabinovich (1997) and Monserrat *et al.* (1998) made no attempts to apply this approach to examine tsunamis and meteo-tsunamis recorded at the same sites and to compare their source characteristics. The data obtained on the B.C. coast during tsunami and storm events enable us to do this investigation.

Sea level oscillations observed near the coast may be presented as

$$\zeta_{\text{obs}}(t) = \zeta_e(t) + \zeta_b(t), \quad (7)$$

where  $\zeta_e$  are the “event” oscillations, (e.g. tsunami waves generated by an underwater seismic source or meteotsunami generated by an atmospheric source), and  $\zeta_b$  are the background surface oscillations. The spectrum of each of these components ( $\zeta_e$ ,  $\zeta_b$ ) may be presented in form (2). In this formulation, we assume that the spectra of the observed extreme events, or of ordinary long waves, are a product of the same topographic admittance function, strongly variable in space (due to the resonant properties of local topography) and almost constant in time, and the corresponding source spectra, locally uniform in space but significantly variable in time. The correctness of this assumption, which is crucial for the proposed approach, may be verified after obtaining the final results.<sup>1</sup>

According to (7), the observed spectrum  $S_{\text{obs}}(\omega)$  may be presented as

$$S_{\text{obs}}(\omega) = S_e(\omega) + S_b(\omega). \quad (8)$$

If we assume that the background noise is the same before and during the event,  $\hat{S}_b(\omega) \approx S_b(\omega)$ , and take into account (3), we get the following expression:

$$R(\omega) = \frac{S_{\text{obs}}(\omega)}{\hat{S}_b(\omega)} = \frac{[E(\omega) + S_0(\omega)]}{\hat{S}_0(\omega)} = A^{-1}\omega^2 E(\omega) + 1.0. \quad (9)$$

The spectral ratio,  $R(\omega)$ , is independent of the location of the station and entirely determined by the forcing. So, it is an invariant characteristic of the source and should be nearly the same for all stations. We will call  $R(\omega)$  the ‘source function’.<sup>2</sup> This function shows relative amplification of the longwave spectrum during the event in comparison with the ordinary situation.

Figures 12 and 13 present the constructed spectral ratios (source functions) for the October 2000 storm and the Peru 2001 tsunami. There are clear differences between the ratios. The Peru tsunami source (Figure 13) is associated with specific frequency bands 0.01–0.2 Hz (periods 5–100 min) with peak values at 0.035–0.1 Hz (10–30 min). This frequency band is typical for tsunami waves (Murty, 1977).



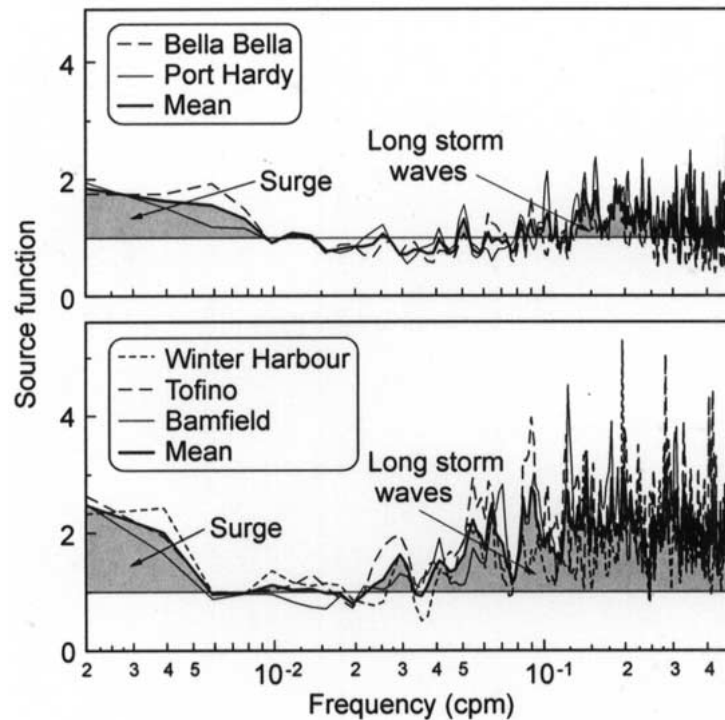


Figure 12. Source functions of the October 2000 storm oscillations on the B.C. coast. Shaded area shows mean zone of the energy pumping.

In contrast, the source function for the long waves associated with the October 2000 storm (Figure 13) is mainly confined to the entire frequency band higher than approximately 0.03–0.07 Hz (periods 15–30 min) and amplifies toward the Nyquist frequency.

Kovalev *et al.* (1991) described very similar storm long wave behaviour on the southwestern shelf of Kamchatka in the Sea of Okhotsk. They found that high-frequency longwave energy increases during storms at periods less than 35–40 min, but remains almost unchanged at lower frequencies. According to the authors, this process is similar to a phenomenon of ‘negative viscosity’ in turbulence, when motions at high frequencies and small scales transfer energy to large-scale, low frequency motions. Hasselman (1971) presented a theoretical mechanism describing energy transfer from short gravity waves to long waves. This non-linear mechanism may occur only in the presence of an intensive external high-frequency source such as energetic storm waves. The long waves associated with non-linear interaction of wind waves are known as ‘infragravity waves’ (Holman *et al.*, 1978; Oltman-Shey and Guza, 1987). High interest in infragravity (IG) waves is due to their important role in beach destruction and transformation (Bowen and Huntley, 1984). Typical periods of IG-waves are 30–300 sec, i.e. sufficiently shorter than tsunami waves. Significant intensification of non-linear processes during severe storms may cause

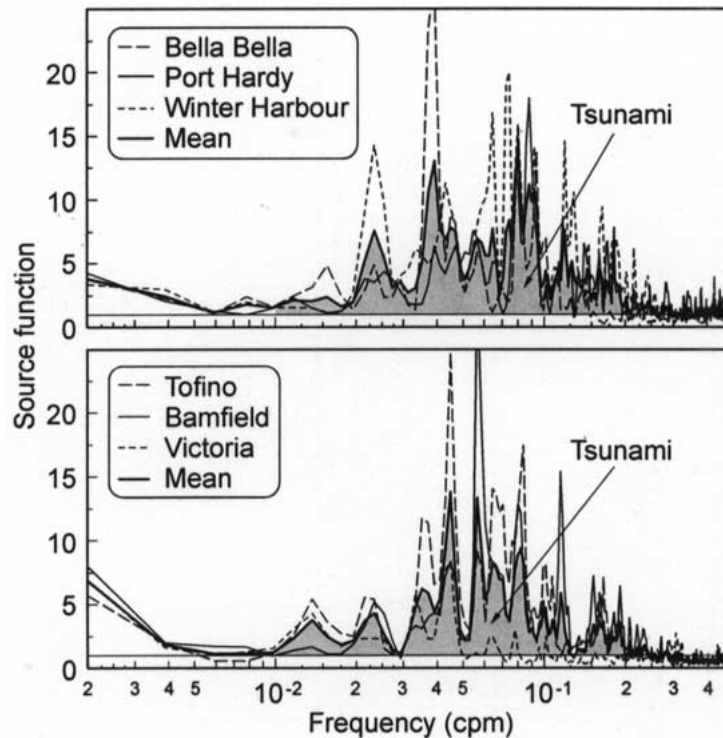


Figure 13. Source functions of the Peru 2000 tsunami oscillations on the B.C. coast. Shaded area shows the mean zone of the energy pumping.

the generation of much lower-frequency IG-waves. Apparently, the presence of the IG-waves, generated by the October 2000 storm, modifies the source function and determines the visible difference between the spectral ratios event/background for storm seiches and tsunami (Figures 12 and 13).

Of course, atmospheric activity generates long waves not only through the non-linear interaction of wind waves, but also directly by dynamic forcing of atmospheric pressure on the sea surface (Rabinovich, 1993). The destructive meteorological tsunamis are mainly related to atmospheric buoyancy waves or pressure jumps and may occur even during calm weather. 'Rissaga waves', catastrophic seiche oscillations in the inlets of Menorca Island, Western Mediterranean, are a classical example (Rabinovich and Monserrat, 1996). In this case, the 'tail' of IG-waves, similar to that seen in Figure 13, will be absent in the source function. However, as was shown by Monserrat *et al.* (1997), the source function of 'rissaga waves' has specific shape, distinguishable from any other types of oscillations. Apparently, the source functions of seismic and meteorological tsunamis are essentially different, but more observational data are considered necessary to support this supposition.

Definition of the tsunami source function during storm weather remains problematic. Apparently, in such situations we should assume that the observed sea level oscillations,  $\zeta_{\text{obs}}(t)$ , constitute the superposition of tsunami waves,  $\zeta_t(t)$ , storm seiches,  $\zeta_s(t)$ , and ordinary background oscillations,  $\zeta_b(t)$ , and use a similar approach to that described above but with division of the observed record into two segments: (1) “pre-tsunami”, with storm seiches but without tsunami waves, and (2) “tsunami”, when all three components exist we would then compare the corresponding spectra to find the difference.

## 7. Concluding Remarks

There are several questions we would like to answer using the present analysis, in particular the following:

- How efficient is the upgraded Tsunami Warning System for the B.C. coast; could relatively small tsunamis be recorded by the tsunami warning stations (Tofino, Winter Harbour, and Langara) as well as by the Permanent Water Level Network (PWLN) stations?
- Is it important to sample once a minute (or more frequently)? What happens if the stations decimate the data recording to 6-minute sample intervals?
- What are the frequency responses of various stations? How strong will the topographic amplification of arriving tsunami waves be at different locations?
- What is the difference in tide gauge response to tsunamis and atmospherically generated waves (meteorological tsunamis)? Can this difference be detected from the data analysis (i.e. without additional information on seismic or meteorological events)?

The data quality from the upgraded PWLN instruments has clearly improved. The digital recording of sea levels has significantly increased the accuracy of long wave collection and made the data processing much easier and efficient. As a result, two recent tsunamis have been recorded and identified. One of them (June 23, 2001) was a distant event with a source area over 10,000 km from the B.C. coast. Nevertheless, all B.C. stations, except those located deeply inland, recorded this tsunami. The observed wave heights were relatively small (from 3.7 cm in Queen Charlotte City to 15.1 cm in Tofino). The tsunami signal was clear and easily distinguishable from the background noise. The October 12, 2001 tsunami was produced by a moderate local earthquake ( $M_w = 6.3$ ). This tsunami, with wave heights 10-20 cm, was recorded by four stations located in the vicinity of the source area (Winter Harbour, Port Hardy, Tofino, and Bamfield). The tsunami signal was quite clear and recognizable. So, the new tide gauge system demonstrates high efficiency to record both far-field (distant) and near-field (local) tsunamis. What is important is that two of the three tsunami warning stations (Tofino and Winter Harbour) recorded both tsunamis and the records are of very good quality.

Unfortunately, there are still serious problems with the third tsunami warning station, Langara. This station is important if there is to be an efficient tsunami

warning system for the B.C. coast because it is located at the closest distance from a region of high tsunami risk – the Alaska–Aleutian seismic zone. Installation of a tsunami gauge on Langara Island was a technical challenge: several times in the past the sensor and the instrument shelter were carried away or damaged by strong waves during storms, which in this area are frequent and violent (Rapatz and Murty, 1987). At the moment tides at this station are recorded relatively well but, as the present analysis showed, long waves in the tsunami frequency band are strongly distorted either because of the sensor problems or due to unfortunate gauge position. Also, the Langara station is known to have frequent operational problems, in particular, the station did not work during the October 2000 storm and the Queen Charlotte tsunami. Improvement of this station needs to be high priority.

Once a tsunami has occurred, it is important to observe it at as many sites as possible. The PWLN stations from this point of view are very valuable. For measuring Pacific tsunamis the most important stations are those located on or close to the outer coast. Bamfield and Port Hardy recorded both the Peru and Queen Charlotte tsunamis, and the qualities of these records were quite high. The Victoria tide gauge located in Juan de Fuca Strait was too far away from the epicenter of the Queen Charlotte earthquake and did not measure the resultant tsunami, however it recorded the Peru tsunami. All these stations, as well as the tsunami warning stations at Tofino and Winter Harbour, are located on the coast of Vancouver Island. Unfortunately, there are no appropriate tsunami stations on the northern coast of British Columbia. Queen Charlotte City is strongly shielded from arriving tsunami waves, Bella Bella is located too far inland (both stations recorded the Peru tsunami, but the signal was weak in comparison with the Vancouver Island stations). The topographic admittance characteristic of the Prince Rupert station was found to prevent recording tsunami waves (probably due to the instrument location). That is why neither of the two tsunamis was observed at this station. So, a reliable northern tsunami station is still a problem to solve.

Decimating the data recording to 6-minute sample intervals would reduce some expenses and simplify the data storage. However, the Nyquist period in that case will become 12 min. As indicated by Figure 7, the major topographic admittance peaks at most stations are located at periods less than 12 min. Thus, decimating the sample interval to 6 min would deprive us of important information about long waves in the tsunami frequency band and may create serious aliasing problems (cf. Emery and Thomson, 2001). This can be painlessly done only for the stations Prince Rupert, Point Atkinson and probably Campbell River. At the same time, there is no apparent reason to reduce this interval to 30 or 15 sec; this can be important for investigation of IG-waves, but is not so crucial for tsunami waves.

Most of the tsunami and PWLN stations are located in bays, inlets and fjords of the B.C. coast having distinct resonant properties. The frequency response at various stations (in particular at Winter Harbour, Tofino, Bamfield, Port Hardy, and Victoria) is strong and clear. The corresponding resonant periods are relatively

short (from 2.5 to 20 min), demonstrating the major impact for these stations in the event of relatively high-frequency tsunami. In the case of resonance, the arriving waves at these locations may amplify 10–15 times. The Winter Harbour station also has two strong resonant peaks with periods of 30 and 47 min and with amplification factors of about 7. The expected periods of arriving tsunami waves may be roughly estimated based on the source dimensions and ocean depth in the source area (Rabinovich, 1997). Hence, in principal, it is possible to predict the respective impact of arriving waves at different locations.

The difference in tide gauge response to tsunamis and atmospherically generated waves is probably the most difficult to determine. However, results presented in the previous section are very encouraging and suggest that this problem can also be solved.

### Acknowledgements

The authors would like to thank Denny Sinnott for his great help with acquiring the data and Rick Thomson for useful discussions and valuable comments. This research was partially sponsored by the Canadian Hydrographic Service.

### Notes

<sup>1</sup> In fact this assumption is very similar to that which is used as the basis of the harmonic analysis of tides: Every tidal constituent (with a fixed frequency) is presented as a product of two complex magnitudes, astronomical, depending only on time and independent on space, and tidal harmonic, constant in time but variable in space [cf. Pugh, 1987].

<sup>2</sup> A source function defined in this way is always *positive* in contrast to  $E(\omega)/\hat{S}_0(\omega) = R(\omega) - 1.0$ , which can be negative at some frequencies when  $S_{\text{obs}}(\omega) < \hat{S}_b(\omega)$  (see Figure 10).

### References

- Aida, I., Hatori, T., Koyama, M., Nagashima, H., and Kajiura, K.: 1972, Long-period waves in the vicinity of Onagawa Bay. (I) Field measurements in Onagawa and Okachi bays, *J. Oceanor. Soc. Japan* **28**, 207–219.
- Bernard, E. N.: 1998, Program aims to reduce impact of tsunamis on Pacific states, *EOS* **79**(22), 258, 262–263.
- Bowen, A. J. and Huntley, D. A.: 1984, Waves, long waves and nearshore morphology, *Marine Geology* **60**, 1–13.
- Clague, J. J.: 2001, Tsunamis, In: G. R. Brooks (ed.), *A Synthesis of Geological Hazards in Canada*, Geol. Surv. Canada, Bull. 548, pp. 27–42.
- Clague, J. J. and Bobrowsky, P. T.: 1999, The geological signature of great earthquakes off Canada's west coast, *Geoscience* **26**(1), 1–15.
- Clague, J. J., Munro, A., and Murty, T. S.: 2003, Tsunami hazard and risk in Canada, *Natural Hazards* **28**(2–3), 407–434.
- Defant, A.: 1961, *Physical Oceanography*, Vol. 2, Pergamon Press, Oxford, UK.
- Emery, W. J. and Thomson, R. E.: 2001, *Data Analysis Methods in Physical Oceanography*, 2nd and Revised Edition, Elsevier, Amsterdam, 638 pp.

- Evans, S. G.: 2001, Landslides, In: G. R. Brooks (ed.), *A Synthesis of Geological Hazards in Canada*, Geol. Surv. Canada, Bull. 548, pp. 43–79.
- Filloux, J. H., Luther, D. S., and Chave, A. D.: 1991, Update on seafloor pressure and electric field observations from the north-central and northeastern Pacific, In: B. B. Parker (ed.), *Tidal Hydrodynamics*, J. Wiley, New York, pp. 617–639.
- Geist, E. L., Kikuchi, K., Hirata, K., Yoshioka S., and Bilek, S.: 2001, Modeling the 23 June 2001 Peru local tsunami using results from a quick seismic inversion of the earthquake, In: *Intern. Tsunami Symp. 2001*, Seattle, WA, Proceedings, CD, pp. 411–412.
- González, F. I., Satake, K., Boss, E. F., and Mofjeld, H.: 1995, Edge wave and non-trapped modes of the 25 April 1992 Cape Mendocino tsunami, *Pure Appl. Geophys.* **144**, 409–426.
- González, J. I., Fareras, S. F., and Ochoa, J.: 2001, Seismic and meteorological tsunami contributions in the Manzanillo and Cabo San Lukas seiches, *Marine Geodesy* **24**, 219–227.
- Goring, D. G.: 2002, Response of New Zealand waters to the Peru tsunami of 23 June 2001, *N.Z. J. Mar. Freshw. Res.* **36**, 225–232.
- Hasselmann, K.: 1971, On the mass and momentum transfer between short gravity waves and large-scale motions, *J. Fluid Mech.* **50**, 189–205.
- Hebenstreit, G. T. and Murty, T. S.: 1989, Tsunami amplitudes from local earthquakes in the Pacific Northwest Region of North America. Part 1: The outer coast, *Marine Geodesy* **13**, 101–146.
- Holman, R. A., Huntley, D. A., and Bowen, A. J.: 1978, Infragravity waves in storm conditions, *Proc. 16th Coastal Eng. Conf.*, Hamburg, pp. 268–284.
- Honda, K., Terada, T., Yoshida, Y., and Isitani D.: 1908, An investigation on the secondary undulations of oceanic tides, *J. College Sci., Imper. Univ. Tokyo*, 108 pp.
- Kovalev, P. D., Rabinovich, A. B., and Shevchenko, G. .: 1991, Investigation of long waves in the tsunami frequency band on the southwestern shelf of Kamchatka, *Natural Hazards* **4**, 141–159.
- Kulikov, E. A., Rabinovich, A. B., Spirin, A. I., Poole, S. L., and Soloviev, S. L.: 1983, Measurement of tsunamis in the open ocean, *Marine Geodesy* **6**(3–4), 311–329.
- LeBlond, P. H. and Mysak, L. A.: 1977, *Waves in the Ocean*, Elsevier, Amsterdam, 602 pp.
- Miller, G. R.: 1972, Relative of tsunamis, *Hawaii Inst. Geophys.*, *HIG-72-8*, 7 pp.
- Miller, G. R., Munk, W. H., and Snodgrass, F. E.: 1962, Long-period waves over California's continental borderland, II, Tsunamis, *J. Mar. Res.* **20**(1), 31–41.
- Mofjeld, H. O., González, F. I., and Newman, J. C.: 1999, Tsunami prediction in U.S. coastal regions, In: C. N. K. Mooers (ed.), *Coastal Ocean Prediction*, Coastal and Estuarine Studies 56, AGU, Washington, pp. 353–375.
- Mofjeld, H. O., González, F. I., Bernard, E. N., and Newman, J. C.: 2000, Forecasting the heights of later waves in Pacific-wide tsunamis, *Natural Hazards* **22**, 71–89.
- Monserrat, S., Rabinovich, A. B., and Casas, B.: 1998, On the reconstruction of the transfer function for atmospherically generated seiches, *Geophys. Res. Lett.* **25**(12), 2197–2200.
- Murty, T. S.: 1977, *Seismic Sea Waves – Tsunamis*, Bull. Fish. Res. Board Canada 198, 337 pp.
- Murty, T. S.: 1992, Tsunami threat to the British Columbia coast, In: *Geotechnique and Natural Hazards*, BiTech. Publ., Vancouver, BC, pp. 81–89.
- Okal, E. A., Araya, S., Borrero, J. C., Dengler, L., Gomer, B. M., Koshimura, S., Laos, G., Olese, D., Ortiz, M., Swensson, M., Titov, V. V., and Vegas, F.: 2001, The Peruvian tsunami of 23 June 2001: Preliminary report by the International Tsunami Survey Team, In: *Intern. Tsunami Symp. 2001*, Seattle, WA, Proceedings, CD, pp. 377–378.
- Oltman-Shey, J. and Guza, R. T.: 1987, Infragravity edge wave observations on two California beaches, *J. Phys. Oceanogr.* **17**(5), 644–663.
- Pugh, D. T.: 1987, *Tides, Surges, and Mean Sea-Level*. J. Wiley, Chichester, 472 pp.
- Rabinovich, A. B.: 1993, *Long Ocean Gravity Waves: Trapping, Resonance, and Leaking* (in Russian), Gidrometeoizdat, St. Petersburg, 325 pp.
- Rabinovich, A. B.: 1997, Spectral analysis of tsunami waves: Separation of source and topography effects, *J. Geophys. Res.* **102**(C6), 12,663–12,676.

- Rabinovich, A. B. and Monserrat, S.: 1996, Meteorological tsunamis near the Balearic and Kuril Islands: Descriptive and statistical analysis, *Natural Hazards* **13**(1), 55–90.
- Rabinovich, A. B., Kulikov, E. A., and Thomson, R.E.: 2001, Tsunami risk estimation for the coasts of Peru and northern Chile, In: *Intern. Tsunami Symp. 2001*, Seattle, WA, Proceedings, CD, pp. 281–291.
- Rabinovich, A. B., Thomson, R. E., Bornhold, B. D., Fine, I. V., and Kulikov, E. A.: 2003, Numerical modelling of tsunamis generated by hypothetical landslides in the Strait of Georgia, British Columbia, *Pure Appl. Geophys.* **160**(7), 1273–1313.
- Raichlen, F., Lepelletier, T. G., and Tam, C. K.: 1983, The excitation of harbors by tsunamis, In: K. Iida and T. Iwasaki (eds), *Tsunamis – Their Science and Engineering*, Terra Sci., Tokyo, pp. 359–385.
- Rapatz W. J. and Murty, T. S.: 1987, Tsunami warning system for the Pacific coast of Canada, *Marine Geodesy* **11**, 213–220.
- Subbotina, M. M., Thomson, R. E., and Rabinovich, A. B.: 2001, Spectral characteristics of sea level variability along the west coast of North America during the 1982–83 and 1997–98 El Niño events, *Progress in Oceanography* **49**, 353–372.
- Thomson, R. E.: 1981, *Oceanography of the British Columbia Coast*, Can. Spec. Publ. Fish. Aquat. Sci. 56, Ottawa, 291 pp.
- Wigen, S. O.: 1983, Historical studies of tsunamis at Tofino, Canada, In: K. Iida and T. Kawasaki (eds), *Tsunamis – Their Science and Engineering*, Terra Sci. Publ. Comp., Tokyo, Japan, pp. 105–119.
- Wigen, S. O. and White, W. R. H.: 1964, Tsunami of March 27–29, 1964, west coast of Canada, Unpublished manuscript, Department of Mines and Technical Surveys, Ottawa, 6 pp.

